

In Situ Gelling Polysaccharide-Based Hydrogel for Cell and Drug Delivery in Tissue Engineering

Yixing Cheng,¹ Ahmed A. Nada,^{2,3} Chandra M. Valmikinathan,¹ Paul Lee,¹ Danni Liang,¹ Xiaojun Yu,¹ Sangamesh G. Kumbar^{2,3,4,5}

¹Department of Chemistry, Chemical Biology and Biomedical Engineering, Stevens Institute of Technology, Hoboken, New Jersey 07030

²Raymond and Beverly Sackler Center for Biomedical, Biological, Physical and Engineering Sciences, University of Connecticut Health Center, Farmington, Connecticut 06030

³Department of Orthopaedic Surgery, University of Connecticut Health Center, Farmington, Connecticut 06030

⁴Institute for Regenerative Engineering, University of Connecticut Health Center, Farmington, Connecticut 06030

⁵Department of Materials and Biomedical Engineering, University of Connecticut, Storrs, Connecticut 06269

Correspondence to: S. G. Kumbar (E-mail: kumbar@uchc.edu)

ABSTRACT: Injectable hydrogels have attracted a great deal of attention as cell carriers and bioactive agents in regenerative medicine due to their ability to fill complex three-dimensional (3D) tissue gaps and relative ease of *in vivo* administration. Polysaccharide-based hydrogels can provide microenvironments that favor tissue regeneration and biocompatibility due to their chemical similarities with native extracellular matrix components. This manuscript reports the *in vitro* application of an injectable chitosan-based polysaccharide hydrogel for cell and protein delivery. Crosslinked hydrogels were produced by the reaction between the amino functionality of chitosan and the aldehyde of dextran aldehyde resulting in an imine bond (Schiff's base) formation in aqueous solutions. This approach eliminated the use of additional crosslinking agents which may pose undesired side effects regarding cytotoxicity and biocompatibility. Additionally, we demonstrate versatility of the gel in terms of its fabrication, and ability to alter mechanical properties by changing the crosslinking extent due to aldehyde content. Bovine serum albumin (BSA), used as a model protein, followed a steady release pattern from the gel. BSA release was dependent on the extent of hydrogel crosslinking. Increase in crosslinking extent resulted in improved mechanical properties and sustained release of BSA. Human fetal osteoblasts encapsulated into the hydrogel showed at least 70% viability and continued to proliferate under *in vitro* culture. © 2013 Wiley Periodicals, Inc. *J. Appl. Polym. Sci.* **2014**, *131*, 39934.

KEYWORDS: gels; biodegradable; biomaterials; drug delivery systems; polysaccharides

Received 31 July 2013; accepted 3 September 2013

DOI: 10.1002/app.39934

INTRODUCTION

In situ gelling hydrogels could potentially alleviate several drawbacks associated with contemporary regenerative medicine approaches and scaffolds. Primarily, they minimize the invasiveness of the open surgical technique¹ and can conform to complex 3D geometries.² This is critical in repair of trauma and regeneration post-tumor resection. More importantly, this allows for delivery of cells and growth factors locally, which could potentially lead to faster and complete regeneration.³ Most *in situ* gelling hydrogels are composed of extracellular matrix (ECM) proteins and analogs, which integrate well with the host tissues and guide the repair process effectively.⁴ However, natural ECM molecules or proteins, such as collagen, are hard to purify and may lose their biological activity post-processing. Additionally, allogeneic proteins may carry a potential

risk of inflammatory response and disease transmission.⁵ Synthetic polymers or other polymers of natural origin could alleviate the previously mentioned drawbacks while providing a template for easy modification to include cell-recognizable proteins or peptides or a blank slate for deposition of cellular proteins after delivery *in vivo*.⁶

Abundance of chemically reactive functional groups on the natural polymers offers opportunities to dissolve and crosslink the polymer network into 3D stable networks.⁷ Most common physiochemical crosslinking methods to achieve *in situ* gelation includes photochemical or ultraviolet (UV) light crosslinking,^{8,9} molecular self-assembly,^{10,11} and electrostatic interactions.¹² Chemically crosslinked, *in situ* gellable systems have several advantages as compared to photopolymerizable hydrogels; like being devoid of cytotoxic photoinitiators and potentially

harmful exposure to UV radiation.^{8,9} On the other hand, electrostatically or ionically crosslinked hydrogels generally have weaker mechanical properties, uncontrollable swelling and growth factor release kinetics, thus impeding their application.¹³ Chemically crosslinked polysaccharide-based hydrogels often utilize crosslinking agents such as carbodiimide,¹⁴ glutaraldehyde,¹⁵ or adipic dihydrazide¹⁰ to retain shape and enhance mechanical properties.¹¹ However, these crosslinking agents may pose undesired side effects including cytotoxicity and biocompatibility. In recent years focus has been made to create polymeric systems that can produce hydrogels without the use of toxic crosslinking agents for cell and bioactive factor delivery. Majority of these studies are focused on improving gelation time and mechanical strength suitable for tissue regeneration applications.⁷

Chitosan the second most abundant organic material next to cellulose has many advantages over other polysaccharides, due to its nontoxicity and biodegradability, as it is broken down in the human system to harmless products (amino sugars) that can be easily absorbed.^{16,17} Additionally, chitosan has several active functional groups that allow for protein binding and an inherent positive charge that is known to stimulate cell interactions and differentiation.¹⁸ The low pH solubility of chitosan may pose limitations in terms of cell and growth factor encapsulation for regenerative medicine applications. A water-soluble derivative of chitosan, carboxymethyl chitosan (CMC) is widely used for drug delivery and tissue engineering applications.¹⁹ Chitosan and its derivatives are often processed into desirable structures and these structures are stabilized by glutaraldehyde²⁰ or genipin²¹ like crosslinkers. However, the biological acceptance of such crosslinked products depends upon the amount of crosslinking agent present in the final product.²² It has been noted that the reason for cytotoxicity of the aldehyde terminated crosslinkers, is the smaller molecular weight, which leads to intracellular permeation and crosslinking of internal proteins.²³ Therefore, high molecular weight crosslinkers should alleviate this effect. Previously, oxidized dextran has been used as a macromolecular crosslinker to crosslink amine functionalities of the polymer.²⁴ This particular hydrophobic hydrogel system was developed as a barrier membrane to prevent postsurgical adhesion which may not be suitable for cell delivery and tissue regeneration applications.²⁵

The rationale behind the application of CMC–dextran aldehyde (CMC-DA) hydrogels is to actively utilize the critical properties of the polymers by generating *in situ* gelling hydrogels via imine bond formation (Schiff base reaction).²⁶ This should potentially yield a biocompatible hydrogel for tissue engineering applications as well as local delivery of either cells or drugs in a controlled manner.

MATERIALS AND METHODS

Materials

Chitosan (190–310 kDa, 75–85% deacetylated), dextran (from *Leuconostoc sp.*, 500 kDa), chloroacetic acid, sodium periodate (NaIO₄), *tert*-butyl carbazate (tBc), trinitrobenzene sulfonate (TNBS) and bovine serum albumin (BSA) were purchased from Sigma-Aldrich (St. Louis, MO). Dialysis tubing was purchased

from Carolina Biologicals (Burlington, NC) with a molecular weight cut-off at 13,000 Da. CellTiter 96 nonradioactive cell proliferation assay (MTS) was obtained from Promega (Madison, WI). Bradford protein assay kit was obtained from Bio-Rad (Hercules, CA). Live/Dead staining kit was obtained from Invitrogen (Carlsbad, CA).

Cell Culture

Human fetal osteoblast cells (hFOB 1.19, ATCC, Manassas, VA) at Passages 7–8 were used to measure cellular responses following encapsulation in the CMC-DA hydrogel. The choice of osteoblasts was based on their intended bone healing application. Cells were cultured in Dulbecco's modified Eagle's medium-low glucose (DMEM-LG, Cellgro, Manassas, VA) supplemented with antibiotic solution (1% penicillin–streptomycin, Atlanta Biologicals, Lawrenceville, GA), 10% fetal bovine serum (FBS, Atlanta Biologicals, Lawrenceville, GA).

Synthesis of CMC

CMC was prepared by the method previously reported with slight modifications.²⁷ In brief, chitosan (6 g) was magnetically stirred in a mixture of 20 mL sodium hydroxide (10 g, 50% w/v) and 80 mL isopropyl alcohol to swell and alkalinize. The mixture was stirred and heated up to 60°C for 1 h. To this, chloroacetic acid (9 g) dissolved in isopropyl alcohol (20 mL) was added drop-wise and the reaction was allowed for 4 h at the same temperature. The insoluble reaction mixture was filtered and rinsed with isopropyl alcohol. The filter cake was rehydrated with deionized (DI) water (300 mL). Sodium CMC salt solution was neutralized to pH 7.0 using hydrochloride acid (1M) and the insoluble components were separated by centrifugation at 4000 rpm for 10 min (Eppendorf centrifuge 5810R). The CMC was precipitated from supernatant by adding excess amount of cold isopropanol. Crude product was filtered, rinsed with isopropanol, air-dried and then re-dissolved in 300 mL DI water. CMC solution was further purified using dialysis tubing against DI water for 3 days. DI water was replaced every day. The CMC solution was then lyophilized overnight (Labconco, Freeze dry system 4.5) and stored in dark until use.

Determination of Degree of Substitution

The degree of substitution (DS) of CMC was measured by potentiometric titration using well established protocols.^{28,29} In brief, 0.2 g CMC was dissolved in DI water (40 mL) and the pH was adjusted to less than 2. The solution was titrated with 0.1M aqueous NaOH. The pH and potential change were recorded along the process of titration. The amount of NaOH solution was determined by the second order differential method and DS was calculated according to the following equation. These potentiometric titrations were performed in triplicate. In the following equation, *V*, *C*, and *m* denotes volume, concentration, and weight, respectively.

$$DS = \frac{161 \times V_{\text{NaOH}} \times c_{\text{NaOH}}}{m_{\text{CMC}} - 58 \times V_{\text{NaOH}} \times c_{\text{NaOH}}}$$

Synthesis of DA

DA was prepared using oxidative cleavage, based on previously reported protocols.³⁰ In brief, 2.5 g dextran was dissolved in 100 mL DI water. After complete dissolution, sodium periodate

Table I. Gelation Time and Compressive Modulus are Both Concentration and Ratio Dependent

Concentration (w/v)	DA : CMC	Gelation time (s) ^a	Compressive modulus (kPa) ^b
3%	5 : 5	16.1 ± 1.15	21.43 ± 4.15
2%	7 : 3	40.5 ± 4.35	5.66 ± 0.45
2%	5 : 5	51.2 ± 12.0	8.07 ± 0.41
2%	3 : 7	37.5 ± 2.64	5.63 ± 1.03

^aFor each group, six samples ($n = 6$) were counted and averaged. Results were reported as mean ± SD.

^bDetails for calculation of compressive modulus are described in mechanical test section.

(1.65 g) was added under agitation. Reaction mixture was stirred and allowed to react overnight protected from light. One milliliter of ethylene glycol was added drop wise to quench the reaction for an hour by consuming excessive periodate. The quenched reaction mixture was dialyzed immediately against DI water for 3 days with daily DI water changes followed by lyophilization. The synthetic details and aldehyde group stability as well as its susceptibility to protonation have been elucidated elsewhere.^{31,32}

Determination of Degree of Oxidization of DA

The degree of oxidization (DO) of DA was determined using a TNBS titration method, as described previously.³⁰ The DO of DA is defined as the number of oxidized residues per 100 glucose residues. Typically, DA solution (5 mL, 0.01M) and *tert*-butyl carbazate (tBC, 5 mL, 0.03M) were mixed in aqueous trichloroacetic acid (1%) and stirred overnight. Two hundred microliters of reaction mixture was aliquoted into a vial containing TNBS solution (1 mL, 85.5 mM in phosphate buffer). After 1-hour reaction, absorbance at 334 nm was measured using a microplate reader (Biotek Instruments) and the value was fitted into a pre-established standard curve.

Preparation of CMC-DA Hydrogel

Lyophilized CMC and DA powder were reconstituted in phosphate buffered saline (PBS, 0.01M, pH = 7.4) to form 1.0%, 2.0%, 3.0% (w/v) solution of each, respectively. Series of solutions were stored at 4°C until used. Hydrogel was formed by mixing DA solution and CMC solution at desired ratios under room temperature. Unless otherwise specified, hydrogels were fabricated in wells of 24-well plate with a total volume of 800 μ L. The gels were mixed well to ensure homogeneity

followed by 10 min of incubation at room temperature to allow complete gelation.

Gelation Time

Gelation time was determined by inverted tube test method. In brief, 800 μ L of hydrogel was made from different combinations of CMC and DA with different concentrations, ratios and DOs, as summarized in Tables I and II, in a glass vial. During the process of gelation, gel-containing vial was inverted time to time to observe solidification. When no significant movement in the gel interface was observed, the time was recorded as gelation time ($n = 6$).

Characterization of Hydrogel Precursors and Hydrogel

Syntheses of CMC, DA, and CMC-DA hydrogel were verified by FTIR (Paragon, Perkin Elmer) at a resolution of 4 cm^{-1} and 64 scans. Lyophilized samples were powdered, mixed with potassium bromide (KBr) and pressed into pellets manually. Unmodified chitosan and dextran were also examined for comparison. Spectrum data was plotted and analyzed using OMNIC 8.0 software.

Mechanical Testing

To measure the mechanical strength of CMC-DA hydrogel and to evaluate how concentration, ratio and DO affect the mechanical strength, a dynamic material analyzer (RSA III) was employed to test the compressive modulus of various hydrogels following the procedural details published elsewhere.³³ Freshly fabricated cylindrical hydrogel samples measuring 6-mm height and 12-mm diameter were compressed between stainless steel plates using a 50 N load cell at a constant strain rate of 0.10 mm/s until a 60% compressive strain was reached. All given strains and strain rates were referenced to the initial 6-mm height of the specimens and data were analyzed using TA Orchestrator. Tangent compressive moduli of various hydrogels were obtained by fitting the data with a linear equation using origin 8.0 and the obtained slopes were the compressive modulus. Six samples ($n = 6$) for each sample type was measured for statistical analysis.

In Vitro Swelling and Degradation

The equilibrium-swelling ratio (ESR) of various hydrogels was measured by incubating hydrogels in PBS (0.01M, pH 7.4) at 37°C and observing their gravimetric change along the incubation time. In brief, preweighed lyophilized samples (W_d) were placed in wells of 12-well plate and submerged in PBS solution. At specific time points, swollen hydrogels were weighted (W_s) after excess water was blotted with Kim wipes. The swelling

Table II. Gelation Time and Compressive Modulus are also DO Dependent

Used NaIO ₄ (g)	Theoretical degree of oxidization (%)	Degree of oxidization ^a (%)	DA : CMC	Gelation time (s) ^b	Compressive modulus (kPa) ^c
1.65	62.1	59.2 ± 1.4	5 : 5	51.2 ± 12.0	8.07 ± 0.41
1.05	39.5	38.7 ± 0.9	5 : 5	63.3 ± 10.4	6.82 ± 0.58
0.55	20.7	18.9 ± 0.8	5 : 5	75.7 ± 13.6	4.57 ± 0.36

^aDO was determined using aforementioned TNBS assay. For each group, the measurements were in triplicate.

^bFor each group, six samples were counted and averaged. Results were reported as mean ± SD.

^cDetails for calculation of compressive modulus are described in mechanical test section.

behavior was monitored over a time period of 8 days. Swelling ratio Q at each time point were calculated using the equation $Q = (W_s/W_d) \times 100$.

Crosslinked hydrogels made from different ratios and concentrations (2% w/v, CMC : DA: 7 : 3, 5 : 5, 3 : 7, 3% (w/v), CMC : DA: 5 : 5) were lyophilized and their dry weights were recorded in advance. Dried hydrogels were incubated with 2 mL DI water in a shaker (50 rpm) at 37°C and water was changed every other day. At every predetermined time point, samples were taken out and then lyophilized to get the dry weight. Degradation was determined by the weight loss between original weight and degraded weight after incubation. For all these measurements were done in triplicate ($n = 3$).

Cytotoxicity of Hydrogel and Hydrogel Precursors

Cell cytotoxicity of the CMC-DA hydrogel as well as hydrogel precursors were measured using extract method in which preformed hydrogels were extracted by medium to prepare hydrogel extract.³⁴ Then the cell viability was tested by incubating cells with the prepared extract. To sterilize, lyophilized CMC and DA powder were exposed to UV for 30 min in the laminar flow hood before reconstitution in PBS. hFOB cells were employed as the model cell line to evaluate the cytocompatibility. Hydrogel extracts were prepared by soaking various preformed hydrogel (CMC : DA: 7 : 3, 5 : 5, 3 : 7, 1 mL in volume) in 5 mL of the same DMEM from the cell culturing. In the meantime, cytotoxicity of hydrogel precursor solution was also tested by culturing osteoblast cells with 10% (v/v) CMC or DA (2% w/v) solution diluted in DMEM medium. One hundred microliters of hydrogel extract medium or precursor solution containing medium were added to preseeded wells (96-well plate, 5×10^3 cells/well, $n = 6$). Cells cultured with nontreated medium were used as control group. During the period of incubation, extract medium and precursor containing medium were replaced every other day. MTS (3-(4,5-dimethylthiazol-2-yl)-5-(3-carboxymethoxyphenyl)-2-(4-sulfophenyl)-2H-tetrazolium) assay was performed at Days 1, 3, and 7 by adding 20 μ L MTS solution to freshly added medium. After incubation for 3 h at 37°C, 100 μ L incubation mixtures was taken out from each well and the absorbance was read by a microplate reader (BioTek, Synergy HT) at 490 nm.^{35,36}

Proliferation and Viability of Cells Encapsulated in Hydrogels

hFOB cells were used to perform the cell encapsulation assay. After first addition of desired amount of 2% (w/v) DA solution into wells of 96-well plate, equal amount of cell suspension (20 μ L) was added and the cell suspension was stirred to ensure homogenous dispersion of cells. Subsequent addition of desired amount of CMC solution and stirring gave rise to the cell-laden hydrogel which was 120 μ L in volume and the cell density was 1×10^4 cells per hydrogel ($n = 3$). The mixture was incubated for 10 min at 37°C in incubator after which 100 μ L medium was added onto the hydrogel and was changed by fresh medium every half an hour in the first 2 h to equilibrate the hydrogel with cell culture media. This step was essential to provide cells with a homogenous environment within the hydrogel. At each predetermined time point, cell proliferation in hydrogel was examined using MTS assay as described

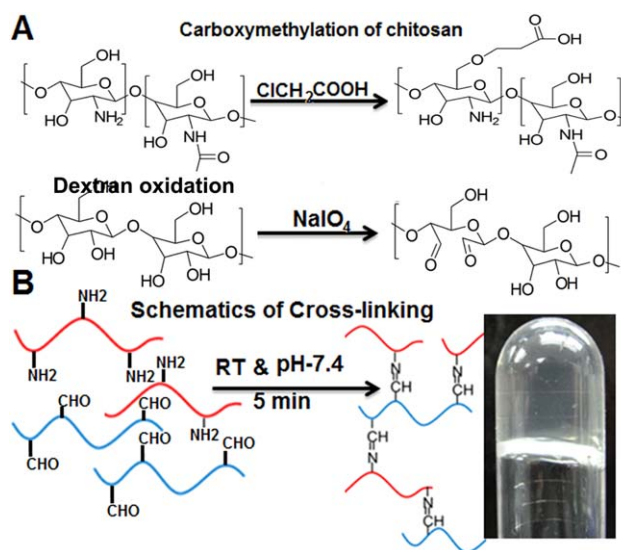


Figure 1. (A) Schematic sketches of carboxymethylation of chitosan, oxidative cleavage of dextran and a macroscopic image of performed CMC-DA hydrogel, (B) illustrative sketch for CMC-DA crosslinking, and a picture of the formed CMC-DA hydrogel in an inverted test tube. [Color figure can be viewed in the online issue, which is available at wileyonlinelibrary.com.]

earlier. For MTS assay, 20 μ L MTS solution was added to newly replaced medium (100 μ L). After 3-h incubation, 100 μ L of formazan dissolved medium was measured in a 96-well microplate for absorbance at 490 nm.

The viability of cells encapsulated in hydrogel was also examined microscopically using Live/Dead staining. For Live/Dead assay, hydrogel/cell constructs (200 μ L in volume, 1×10^5 cells per gel) were fabricated in wells of a 48-well plate as previously described. The cell-laden hydrogels were cultured with 400 μ L medium which was replaced with fresh medium every other day. After 1 day or 1 week of culture, 200 μ L staining solution (SYTO 10 and ethidium homodimer-2 1 : 500 in PBS) was used to incubate the cell-embedded hydrogel for 15 min at room temperature in dark. After staining, cell embedded hydrogels were rinsed with PBS for three times to wash away nonspecific binding of dye as much as possible. Thin cross-section of the stained hydrogel was cut using a razor blade and placed on a glass slides covered with glass slip for visualization under confocal microscopy (Nikon E-1000, C1 CLSM). Cell viability (percentage of green fluorescent cells) was quantified using Image J software by counting live and dead cells in three representative images at constant magnification.

BSA Release from Hydrogels

To examine the potential of CMC-DA hydrogel as drug carrier releasing its payload in a controlled manner, BSA was used as a model protein drug and loaded into the CMC-DA hydrogel. Either CMC or DA lyophilized powder was reconstituted in BSA (2 mg/mL) solution, then 1 mL of CMC-DA hydrogels with different CMC-DA ratios and concentrations (2% w/v: 7 : 3, 5 : 5, 3 : 7, 3% w/v: 5 : 5) loaded with 2 mg BSA were prepared in 15 mL conical tubes. BSA containing hydrogels were

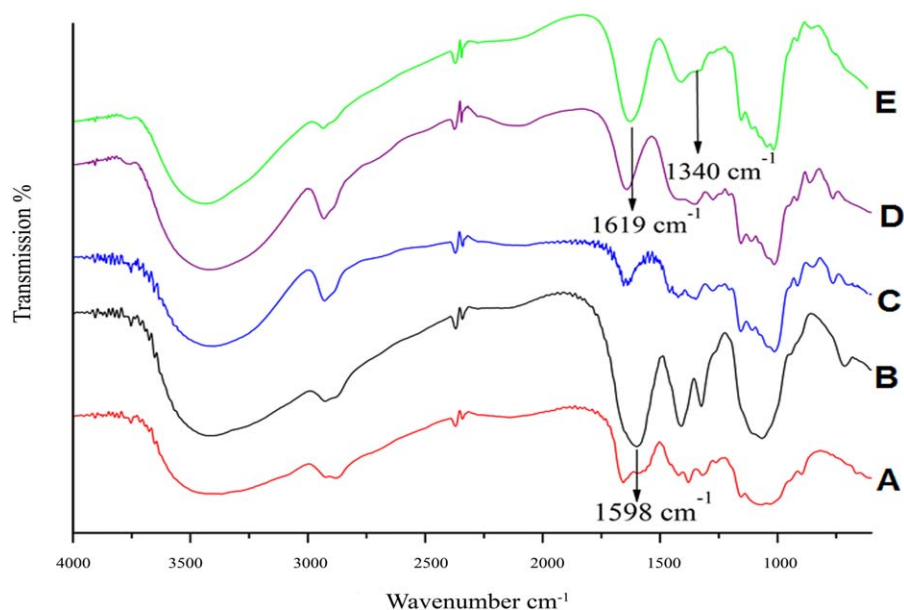


Figure 2. FTIR spectra of chitosan (A), CMC (B), dextran (C), DA (D), and 5 : 5 CMC-DA (E). [Color figure can be viewed in the online issue, which is available at wileyonlinelibrary.com.]

incubated with 1 mL PBS at 37°C in a shaker ($n = 3$). At fixed time intervals, 200 μL released BSA containing PBS was taken out and its protein content was quantified by Bio-Rad protein assay in which absorbance was read at 570 nm.³⁷ The rest of PBS in the conical tube was aspirated out and refilled with fresh PBS.

Statistical Analysis

All quantitative data were recorded as mean \pm standard deviation. Experiment data were analyzed by one-way ANOVA using Origin 8.0 (OriginLab Co., Northampton, MA). A value of $P < 0.05$ was considered to be significant difference.

RESULTS AND DISCUSSION

Characterization of CMC-DA Hydrogel

Schematic illustrations of both modifications of chitosan and dextran are shown in Figure 1(A,B). Modifications on both chitosan and dextran were confirmed by FTIR. Figure 2(A) shows the characteristic peak of chitosan, including at 3428 cm^{-1} (N—H and O—H stretching), 2867 cm^{-1} (C—H stretching), 1650 cm^{-1} (amide I), 1590 cm^{-1} (N—H bending), 1154 cm^{-1} (bridge —O— stretching) and 1083 cm^{-1} (C—O stretching). In the spectrum of CMC [Figure 2(B)], in place of a peak at 1741 cm^{-1} , —COOH appears at 1598 cm^{-1} , in the form of —COONa. An increase in band intensity at 1401 cm^{-1} (—COO[−], symmetric stretching) also confirms the carboxymethylation, meanwhile an increase in band intensity at 1325 cm^{-1} (C—N stretching) proves that carboxymethylation also happened on amine group. Figure 2(C) shows the characteristic spectrum of dextran which is very similar to the spectrum of DA [Figure 2(D)] as the expected peak of aldehyde (1730 cm^{-1}) is not present, due to the formation of hemiacetals.³⁸ Figure 2(E) gives the spectrum of crosslinked CMC-DA hydrogel, the presence of its characteristic peak at 1619 cm^{-1} (C=N, imine stretching) and decrease of magnitude at

1340 cm^{-1} (C—N stretching) demonstrated the formation of Schiff base after crosslinking.^{26,39}

O,N-carboxymethylation of chitosan renders acid soluble chitosan to be soluble at neutral pH while retaining the bioactive amine groups. However, other hydrophilic modifications, such as succinylation, and acrylation⁴⁰ use amino groups thus hindering further *in situ* modification such as growth factor or ECM molecules immobilization. Carboxymethylation enables chitosan derivatives to be amphiphilic, and therefore can respond to pH, which is a prominent characteristic that can be exploited.⁴¹ It was noticed the amino groups in CMC solution either in deionized water or PBS was slightly basic (pH > 7) indicating unprotonated amino acids with negative charge on the macromolecule. The degree of substitution of CMC was determined to be 101% and CMC with this DS was used for other experiments unless specifically mentioned. A DS value higher than 100% was due to multiple carboxymethylations upon one glucose unit.²⁷ The DS of CMC can be controlled over the range of 60–110% by varying the reaction conditions.²⁷ The newly introduced carboxyl functionalities may also be used as additional reactive sites for immobilization of bioactive agents. Bioconjugation of dexamethasone, and RGD peptides through EDC coupling with carboxyl groups on various polysaccharides have been reported recently.⁴²

Vicinal hydroxyl groups in dextran are susceptible to periodate cleavage, generating aldehyde groups after oxidation. Degree of oxidation can be manipulated by varying the amounts of periodate used in the reaction and can readily to be measured by ¹H NMR or TNBS titration. Precipitation formation may complicate NMR readings after reaction between DA and *tert*-butyl carbazate (tBC) due to the bulky butyl group of tBC. For this reason, DO was determined by TNBS assay instead of NMR.³⁰ Under the described reaction condition, the DO of DA was determined to be $59 \pm 1.4\%$ ($n = 3$). By varying the amount of periodate added

in the reaction, DO can be tailored within the range of 10–80%.³⁹ Unless otherwise mentioned, the DA used in this article was 59% oxidized. Aldehyde bearing DA can not only act as a macromolecular crosslinker to form hydrogel with CMC, but also can immobilize other bioactive amino containing molecules via Schiff base formation, thus increasing the biological property of hydrogel. Preliminary evidence for this immobilization was observed in a BSA release experiment in later studies.

By taking advantage of the Schiff base reaction between DA and CMC, a transparent, hydrogel was formed [Figure 1(B)]. Compared to other natural hydrogels such as agarose or alginate systems which might be opaque at different concentrations and crosslinking densities this CMC-DA is colorless and transparent at all concentrations and ratios. This property allows ease in light microscopic analysis.

Gelation time is a crucial property of hydrogel system because slow gelation would cause delocalized gel formation, while fast gelation would clog the syringe before injection. The gelation time of hydrogel is dependent on several factors such as, concentrations of the components, ratio of the components (Table I), and DO of dextran, as shown in Table II. As expected, higher concentration leads to faster gelation and larger compressive modulus, possibly due to the increased presence of amine and aldehyde groups which in turn lead to higher crosslink density. Ratios of CMC to DA also affect gelation and mechanical properties. However, this is not as significant as the effect of change in concentrations of the precursor solutions (CMC and DA). Meanwhile, gelation time is also dependent on the degree of modification on dextran: higher aldehyde presence leads to faster gelation. Summarizing, tunable gelation time opens the possibility of adjusting gelation time to fulfill different requirements in various biomedical applications.

Mechanical Strength

One of the major issues facing contemporary *in situ* gelling hydrogel scaffolds is their weak mechanical strength which leads to fracture postgelation or delocalization of the hydrogel after injection. Higher gelling times often leads to complications including cells settling at the bottom and resulting in inhomogeneous cell and gel distribution. Biomedical applications of hydrogels at different loci demand varying mechanical strength. In this case, a hydrogel with considerable modulus and ability to alter its mechanical properties is highly desired. For CMC-DA hydrogels, unconfined compression testing up to 30% strain showed a linear stress-strain response, although nonlinear parts were found in high strain area. The tangent compressive modulus was determined by the slope of the strain-stress curve and was used as an indicator of the modulus of hydrogels, as described earlier. From the results it can be seen that the hydrogel made from 3% (w/v) precursor solutions was shown to be stiffer than the 2% (w/v) hydrogel, and the hydrogel with 5 : 5 CMC-DA ratio showed better (statistically significant) mechanical stress resistance than other compositions [Figure 3(A)]. In addition, the degree of oxidization of DA also affects the mechanical properties of the hydrogel, since hydrogels made from DA with higher DO were found to be stiffer than hydrogels made from DA with lower DO [Figure 3(B)]. In conclusion, all the differences in mechanical properties are attributed to

the crosslinking density in hydrogels, indicating that the more crosslinks there are in the hydrogel, the stiffer the hydrogel would be. By varying concentration, composition and/or degree of modification, hydrogels with distinct mechanical strength can be obtained to mimic the mechanical strength of natural tissue, such as cartilage⁴³ and intraocular lens,⁴³ for a variety of tissue engineering applications. These injectable hydrogels will be used in conjunction with other mechanically stable scaffolds for load bearing applications.⁴⁴ These injectable hydrogels will be used to deliver cells and factors at the nonload bearing sites.^{45,46} Mechanical properties of these gels are in the range of many other hydrogels developed for similar purposes.^{45,46}

In Vitro Swelling and Degradation

Swelling is one of the unique properties of hydrogels used in biomedical and pharmaceutical applications due to its central role in solute diffusion coefficient, surface properties and

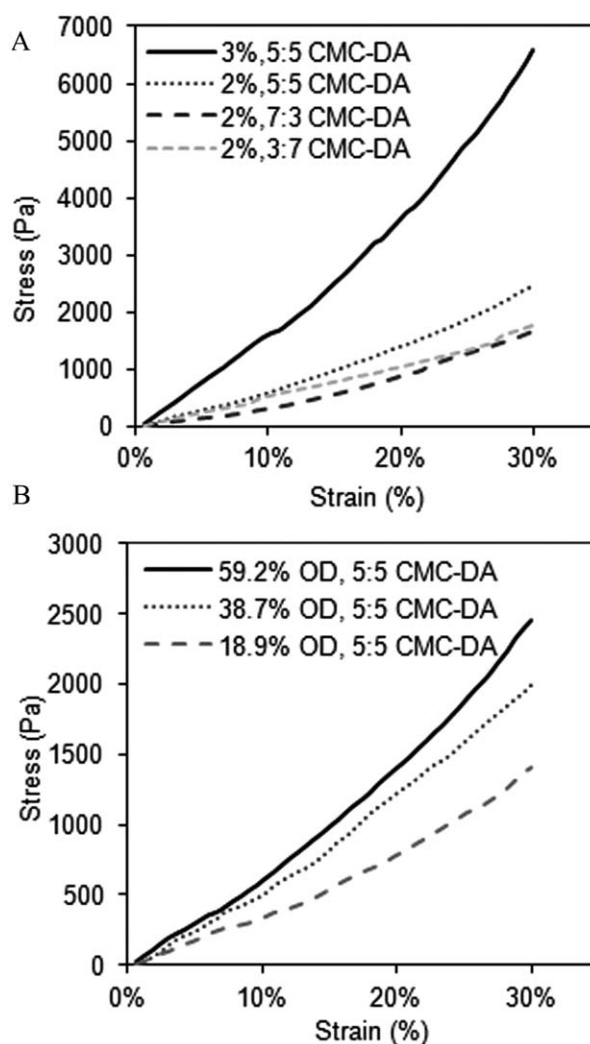


Figure 3. Stress-strain curve of hydrogels under confined compression: (A) Hydrogels composed of different CMC-DA ratios, (B) hydrogel composed of DA with different degrees of oxidization (DO). Tangent compressive modulus of various hydrogels were obtained by fitting the data with a linear equation using Origin 8.0 and the obtained slopes were the compressive modulus.

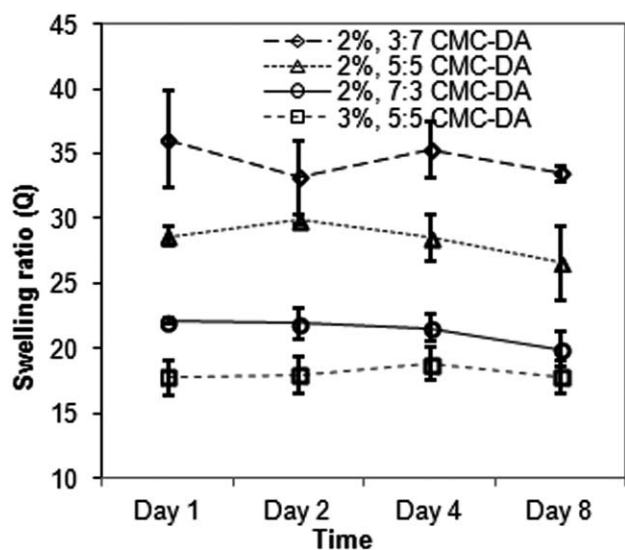


Figure 4. Swelling ratios (Q) of various hydrogels were calculated during a period of 8 days. At each time point, the experiments were in triplicate and were reported as mean \pm SD.

mechanical integrity.⁷ Figure 4 shows the swelling behavior of various hydrogels, revealing that concentration and CMC-DA ratio affect the swelling property of hydrogel. Hydrogels prepared from 3% (w/v) precursor solution showed the lowest swelling ratio (18.79 ± 1.29) as expected, because denser crosslinking results in a smaller internal matrix and/or pore sizes, leading to reduced water diffusion into the matrices. Swelling properties are also CMC-DA ratio dependent as different precursor ratios lead to different swelling ratios. When the CMC content increased from 30 to 70%, the swelling ratio decreased from 36.11 ± 2.83 to 22.13 ± 0.22 . This result indicates that the higher the ratio of CMC in the matrix led to tighter hydrogel construct and hence less water uptake. The density of crosslinking plays a vital role in diffusion of small molecules within the hydrogel. For example, one may limit the diffusion loss of nutritional molecules when a hydrogel is used as cell scaffold, and retain more therapeutic molecules when the hydrogel is used as a drug carrier. Thus, it is advantageous for this hydrogel to have optimal crosslinking densities, based on the application. It is also reasonable enough to believe that degree of modification, DO for DA in this case, can also determine the crosslinking density.

An appropriate biodegradation rate is a desired property of hydrogels, especially for use in tissue engineering applications. Since the imine bonds which crosslink the hydrogel are readily susceptible to hydrolysis, the CMC-DA hydrogel is expected to degrade in a physiological environment.⁴⁷ *In vitro* degradation tests of various hydrogels were carried out up to 16 days in DI water. The reason that it was incubated in DI water instead of PBS is that there was an increased dry weight after incubation with PBS. A hypothesis of this weight increase is that slightly positively charged hydrogel, is likely to absorb oppositely charged inorganic ions that will give additional weight to original hydrogel. As previously alluded, crosslinking density can also determine the rate of degradation, since higher crosslinking density

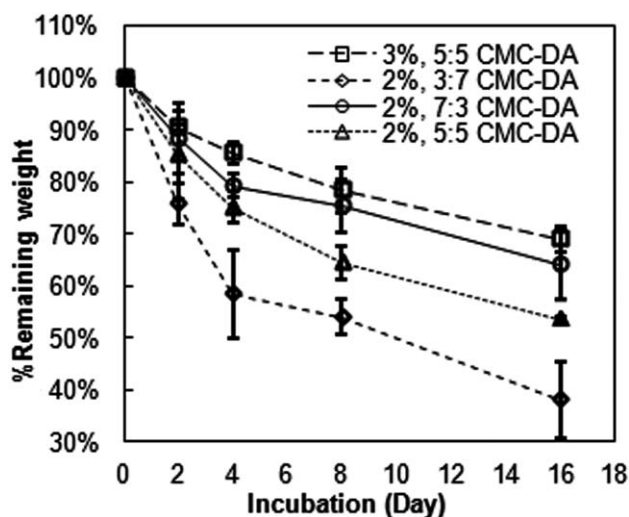


Figure 5. *In vitro* degradation test was carried out in dH_2O over a period of 16 days. Remaining weight percent is the dry weight of sample after incubation to original dry weight of sample. Measurements were in triplicate and results were recorded as mean \pm SD.

consequently decrease the exposure of polymer chains to water molecules, leading to slower weight loss. As Figure 5 illustrated, 3% CMC-DA hydrogel degraded the slowest it has the highest crosslinking index, while 2% 3 : 7 CMC-DA hydrogel degraded faster than others due to least amount of crosslinking. Besides hydrolysis, enzymatic digestion, such as digestion by lysozyme and collagenase, will increase *in vivo* degradation of the hydrogel and thus should be taken into account while performing *in vivo* testing.⁴⁸

Cytotoxicity of Hydrogel and Precursor

Minimal cytotoxicity is the paramount property of a biomaterial and in this case, it is measured by a well-established MTS assay using hFOB cultured with various hydrogel extracts. Hydrogel extracts were prepared by incubating 1 mL performed hydrogel with 5 mL medium at 37°C for 48 h. In the meantime, the cytotoxicity of hydrogel precursor (CMC, DA) solutions (2% w/v) was also measured. The cell viability was examined on Days 1, 3, and 7 as shown in Figure 6. Except on Day 1, where two hydrogel extracts showed increased viability, there was no significant difference between hydrogel extract groups and control groups ($P < 0.05$). This demonstrated that these hydrogels are biocompatible regardless of their compositions. However, cells in 10% (v/v) DA precursor showed mere 70% viability when compared to control. Crosslinking between DA and CMC may inhibit further oxidation and thus render them noncytotoxic to cells. It was also noticed that 3 : 7 CMC-DA hydrogel extract showed higher proliferation than the control group and other two experimental groups. A possible explanation for this phenomenon is that more CMC content has been released via hydrogel degradation in the 3 : 7 hydrogel while CMC is reported, in some cases, to stimulate the extracellular lysozyme activity of cells and promote proliferation.⁴⁹ The results are in agreement with that 3 : 7 CMC-DA hydrogel degraded the fastest, thus more CMC had been extracted in medium. However, 10% (v/v) CMC precursor solution did not

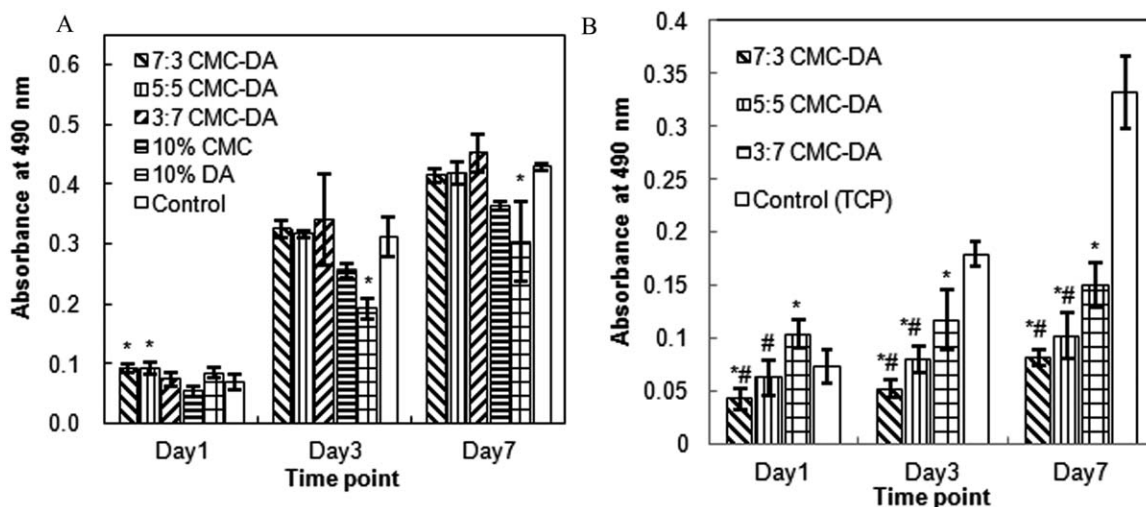


Figure 6. A: Cytotoxicity of hydrogels (CMC:DA, 7 : 3, 5 : 5, 3 : 7) and hydrogel precursor solutions (CMC 10% v/v, DA 10% v/v) were tested using MTS assay, tissue culture plate was used as control and MTS solution added into fresh medium was used as blank ($n = 6$). * denotes group that has a significant difference when compared to control group ($P < 0.05$). B: MTS assay were examined upon cells encapsulated in different hydrogels (CMC : DA, 7 : 3, 5 : 5, 3 : 7) over a period of 1 week, tissue culture plates (TCP) at the same seeding density were used as control ($n = 3$). * indicates that the denoted groups have a significant difference when compared to control group and # indicates that the denoted groups are significantly different from CMC: DA = 3 : 7 group ($P < 0.05$).

assist cell proliferation, alone which demonstrated that the proliferative effect of CMC might be dose-dependent.

Cell Encapsulation in Hydrogels

Encapsulating hFOB3 cells into homogenous CMC-DA hydrogel and measuring the viability of hFOB3 cells entrapped in the hydrogel using both MTS and Live/Dead staining methods validated the potential use of CMC-DA hydrogel as an *in situ* gelling cell scaffold. Except for Day 1, cells cultured on tissue culture plate showed higher proliferation rate than in cell-encapsulated hydrogels. The reason could be multifactorial, such as a negatively charged hydrogel surface that discourages cell attachment, less efficient exchange of nutrients and waste removal, or limited space that prevents cells from spreading therefore altering morphology. Further cells encapsulated in the hydrogel did not grow as much as the control group, proliferation within the hydrogel can be seen in Figure 6(B). It was also shown that the higher DA ratios induce cell proliferation better than the other groups. It seems to be due to the fact that the higher proportions of DA lead to a looser construct, thus allowing nutritional molecules and waste to diffuse more easily, while providing more space for cells. When observed under optical microscopy it was found that the cells entrapped in the hydrogels adopted round-shape morphology, which is typical of all hydrogel-based scaffolds. This is quite distinct from the spindle-like shape when they are spread out on a tissue culture plate, although a small proportion of them still assumed an elongated spindle shape within the hydrogels after longer incubation periods. This is most likely due to cell spreading being inhibited by the dense hydrogel matrix and was less hampered when the hydrogel started degrading.⁵⁰

The viability of encapsulated cells in hydrogel was also examined by Live/Dead assay. By taking advantage of the differential permeability of live and dead cells, SYTO 10 stain nucleic acid of living cells with green fluorescent while ethidium

homodimer-2 labels only dead cells with a compromised membrane. Live/Dead assay was undertaken after 1 day and 1 week of incubation and representative confocal images were captured to showcase the cell viability within the hydrogels [Figure 7(A)]. Overall, observation of these images indicated that most of the cells showed green fluorescence while few cells were red, demonstrating that the CMC-DA hydrogel is not significantly cytotoxic. Quantification of cell viability was performed using ImageJ software to count the percentage of living, green cells out of all cells in three representative images of a specimen. The results [Figure 7(B)] showed that the viability of cells after 1 day in all three different ratios of hydrogels were greater than 90% and no significant difference of cell viability was observed among them, although slightly higher viability was found for 3 : 7 CMC-DA hydrogel. This high cell viability also demonstrated that the *in situ* gelation process did not significantly damage cells and the majority of cells survive post-gelation. Cell viability after long-term culture in hydrogel was around 90%. In the meantime, a slight increase in cellular proliferation was also shown suggesting that cells were still proliferative while in the hydrogel. The high cell viability after either 1 day or 1 week culture showed that the hydrogel is nontoxic in acute (1 day) and chronic (1 week) time frames. The results are consistent with previous metabolic assays reporting that most cells were viable whilst entrapped in CMC-DA hydrogel in a prolonged culture. SYTO 10 green fluorescent dye and ethidium homodimer-2 red fluorescent dye both stain nucleic acid rather than stain the cytoskeletal protein, thus cannot display cell morphology, even though cell spreading which resulted in a spindle like morphology was discovered occasionally under phase contrast microscopy. Presumably, cell encapsulation in hydrogel matrix accelerates the degradation of hydrogel, due to the secretion of degradative enzymes.^{51,52} Crosslinking agent DA may have influence on reactive oxygen species generation *in situ*

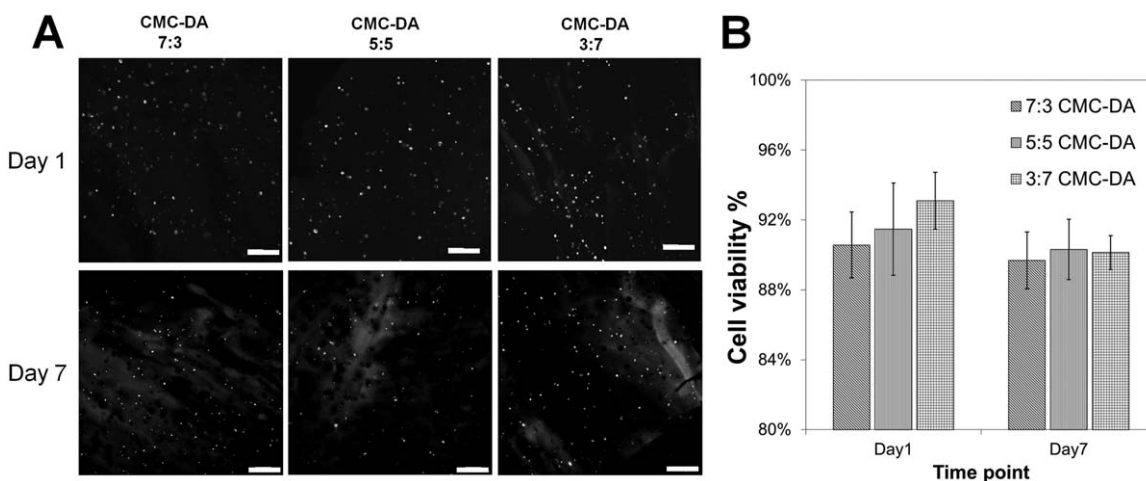


Figure 7. A: Fluorescent images of osteoblast cells encapsulated in various CMC-DA hydrogels either after 1 day or 1 week of incubation. Green and red signals indicate alive and dead cells, respectively. All scale bars indicate 200 μm. B: Cell viability was determined by Live/Dead staining. Three representative fluorescent images for each hydrogel were captured at 10× magnification. Percentage of living cells was calculated by analysing obtained images using Image J software. The values represent mean viability and standard deviation.

when applied *in vivo*.^{53,54} The purpose of this preliminary study was to evaluate the feasibility of cell encapsulation and its delivery. Our future studies plan to characterize this hydrogel system with immune responsive cells, like monocytes, or lymphocytes.

Controlled and Tunable BSA Release from Hydrogels

In this optimization study we have used BSA as a model protein. Often times it is recommended to use BSA as a stabilizing agent for growth factors, making this a relevant model protein. For instance, co-delivery of bioactive small molecules, such as growth factors, and plasmid DNA complexes, along with cells may cause a synergistic effect in therapeutic targets.^{55,56} Thus, the release behavior of CMC-DA hydrogel was investigated. BSA was used as a model protein drug in this study *via* a physical entrapment method. Additionally the possibility of controlling the release profile by deliberate design of composition or concentration of the hydrogel was examined by this experiment. Once a bioactive molecule has been physically entrapped in a biodegradable hydrogel, the release rate primarily depends on: crosslinking density, degradation rate and hydrodynamic kinetics of the small molecule itself.^{57,58} The hydrodynamic diameter of BSA is 7.2 nm, which is much less than the expected mesh size of the CMC-DA hydrogel, so the BSA molecules presumably will diffuse freely within the network.⁵⁹ Figure 8 plots the BSA release profiles from each hydrogel composition. Four distinct phases were observed. A initial burst up to 20% of total BSA was found in every group within the first 6 h which is the first phase, but it is still considerably elevated in comparison with other drug carriers.⁶⁰ The relatively fast release in this stage is probably due to the dissociation of weakly adsorbed BSA on the hydrogel surface. In the second phase which is from 10 to 50 h slower but almost constant release rates were found for each hydrogel. This indicated that the release at this stage is nearly zero-order rate and is presumably dominated by diffusion of BSA and swelling of the hydrogel. Release from 70 to 170 h showed a reduced, but steady rate possibly due to the decreased concentration of BSA. It is reported that release in this stage may be compensated by hydro-

gel degradation. During the last stage, the release became more moderate, even plateauing suggesting that a proportion of BSA was stable in the hydrogel which is a common pattern of other drug delivery systems.⁶¹ BSA is a relatively larger in size than many biological factors including growth factors, peptides and cytokines. These hydrogels may offer a different release profile for smaller sized proteins, cytokines and peptides based on their molecular weight and water solubility. For instance, highly water soluble small molecules will diffuse much faster from the hydrogels as compared to larger molecules with low water solubility.^{62,63} In addition hydrogel crosslinking density has a profound effect on the rate at which encapsulated agents are released.^{64,65} Highly crosslinked polymer networks allow slower release of encapsulated bioactive agents.⁶⁶ These systems can be readily adopted to release a wide variety of bioactive agents.²⁶

From these results, it is reasonable to presume that a faster degradation rate leads to a faster payload release. Instead of performing in accordance with degradation results, BSA release from the 3 : 7

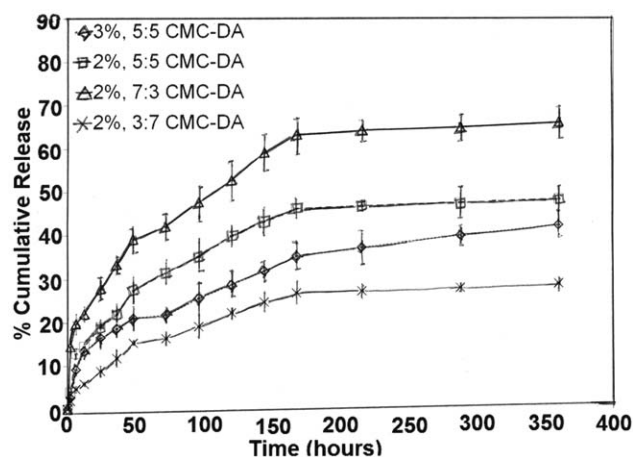


Figure 8. Release profile of BSA from various hydrogel (3%, CMC-DA, 5 : 5; 2% CMC-DA, 7 : 3, 5 : 5, 3 : 7) in PBS at 37°C over 16 days.

CMC-DA hydrogel showed the opposite. When compared to other compositions, 3 : 7 CMC-DA hydrogel showed the slowest BSA release (29% accumulative release after 350 h) even though it degraded the fastest. A hypothetical explanation for this is that N-terminals in soluble BSA can covalently conjugate with excessively available aldehyde groups on DA to form a DA-BSA conjugate via Schiff base formation, therefore hampering the free diffusion of BSA out of the hydrogel matrix. With this being true, a higher DA concentration will retain BSA release in a greater manner. These results further confirmed the possibility of further modification on DA with growth factors or adhesive peptides to increase the biological performance of this hydrogel system.

CONCLUSIONS

In this study, we report the synthesis, fabrication and characterization of a versatile, *in situ* gelling and a tunable hydrogel composed of combination of CMC and oxidized DA. This approach avoids the introduction of any extraneous crosslinking agents, which might be cytotoxic to cells. One of the most important characteristics of this CMC-DA hydrogel system is that all of its properties are tunable. Gelation time, mechanical strength, *in vitro* swelling and degradation can all be tuned to obtain optimal properties for specific biomedical applications by varying the concentrations of the precursors, ratios, and degree of modification. The CMC-DA hydrogel also demonstrated excellent cytocompatibility, as seen by the elution assay as well as cellular staining of encapsulated cells within the hydrogels. The hydrogel can simultaneously act as a drug carrier for proteins or growth factors, which is critical for tissue engineering applications. In addition to tailorability this system minimizes the initial burst release of therapeutics and release rates can be controlled in phases. This CMC-DA hydrogel can be fabricated into a polymeric coating by dipping-dehydration methods or can be chemically modified with a wide variety of bioactive molecules. The active end groups ($-\text{COOH}$ and the $-\text{NH}_2$) have been retained, which allows for further modifications, aiding in the delivery of stem cells and control of their differentiation signals. This system can potentially be applied to a myriad of tissue engineering applications, where cell delivery, survival, differentiation and controlled release are critical.

ACKNOWLEDGMENTS

The authors gratefully acknowledge funding from the Raymond and Beverly Sackler Center for Biomedical, Biological, Physical and Engineering Sciences. They also acknowledge funding from National Science Foundation Award Number IIP-1311907 and EFRI-1332329. They greatly appreciate the help from Dr. Frank Fisher with mechanical testing and Dr. Matthew Libera and his laboratory with confocal imaging.

REFERENCES

- van Tomme, S. R.; Storm, G.; Hennink E. W. *Int. J. Pharm.* **2008**, *355*, 1.
- Peppas, N.; Bures, P.; Leobandung, W.; Ichikawa, H. *Eur. J. Pharm. Biopharm.* **2000**, *50*, 27.
- Leipzig, D. N.; Wylie, G. R.; Kim, H.; Shoichet, S. M. *Biomaterials* **2011**, *32*, 57.
- Glenn P. D. *J. Controlled Release* **2011**, *155*, 193.
- Hennessy, M. K.; Pollot, E. B.; Clem, C. W.; Phipps, C. M.; Sawyer, A. A.; Culpepper, B. K.; Bellis, L. S. *Biomaterials* **2009**, *30*, 1898.
- Fitzpatrick, D. S.; Jafar Mazumder, M.; Lasowski, F.; Fitzpatrick, E. L.; Sheardown, H. *Biomacromolecules* **2010**, *11*, 2261.
- Soppimath, S. K.; Aminabhavi, M. T.; Dave, M. A.; Kumbar, G. S.; Rudzinski, E. W. *Drug Dev Ind Pharm* **2002**, *28*, 957.
- Gutowka, A.; Jeong, B.; Jasionowski, M. *Anat. Rec.* **2001**, *263*, 342.
- McGlohorn, B. J.; Grimes, W. L.; Webster, S. S.; Burg, K. J. L. *J. Biomed. Mater. Res. A* **2003**, *66*, 441.
- Balakrishnan, B.; Jayakrishnan, A. *Biomaterials* **2005**, *26*, 3941.
- Moffat, L. K.; Marra, G. K. *J. Biomed. Mater. Res. B: Appl. Biomater.* **2004**, *71*, 181.
- Schillemans, P. J.; Verheyen, E.; Barendregt, A.; Hennink, E. W.; van Nostrum, C. F. *J. Controlled Release* **2011**, *150*, 266.
- Hoare, T. R.; Kohane, S. D. *Polymer* **2008**, *49*, 1993.
- Rafat, M.; Li, F.; Fagerholm, P.; Lagali, S. N.; Watsky, A. M.; Munger, R.; Matsuura, T.; Griffith, M. *Biomaterials* **2008**, *29*, 3960.
- Ji, C.; Khademhosseini, A.; Deghani, F. *Biomaterials* **2011**, *32*, 9719.
- Jayakumar, R.; Chennazhi, K.; Muzzarelli, R.; Tamura, H.; Nair, S.; Selvamurugan, N. *Carbohydr. Polym.* **2010**, *79*, 1.
- Kim, Y. I.; Seo, J. S.; Moon, S. H.; Yoo, K. M.; Park, Y. I.; Kim, C. B.; Cho, S. C. *Biotechnol. Adv.* **2008**, *26*, 1.
- Richardson, M. S.; Hughes, N.; Hunt, A. J.; Freemont, A. J.; Hoyland, A. *J. Biomaterials* **2008**, *29*, 85.
- Jayakumar, R.; Prabakaran, M.; Nair, S.; Tokura, S.; Tamura, H.; Selvamurugan, N. *Progr. Mater. Sci.* **2010**, *55*, 675.
- Kurihara, H.; Nagamune, T. *J. Biosci. Bioeng.* **2005**, *100*, 82.
- Tan, H.; Marra, G. K. *Materials* **2010**, *3*, 1746.
- Close, M. D.; Patterson, S. S.; Ripp, S.; Baek, J. S.; Sanseverino, J.; Sayler, S. G. *PloS One* **2010**, *5*, e12441.
- Iffiu-Soltész, Z.; Wanecq, E.; Lomba, A.; Portillo, P. M.; Pellati, F.; Szöko, É.; Bour, S.; Woodley, J.; Milagro, I. F.; Alfredo Martinez, J. *Pharmacol. Res.* **2010**, *61*, 355.
- Liu, G.; Shi, Z.; Kuriger, T.; Hanton, R. L.; Simpson, J.; Moratti, S.; Robinson, H. B.; Athanasiadis, T.; Valentine, R.; Wormald, J. P.; Robinson, S. *Macromolecular Symposia* **2009**, *279*, 151.
- Massia, P. S.; Stark, J.; Letbetter, S. D. *Biomaterials* **2000**, *21*, 2253.
- Kumbar, G. S.; Kulkarni, R. A.; Aminabhavi, M. *J. Microencapsul* **2002**, *19*, 173.
- Chen, G. X.; Park, J. H. *Carbohydr. Polym.* **2003**, *53*, 355.
- Yin, L.; Zhao, X.; Cui, L.; Ding, J.; He, M.; Tang, C.; Yin, C. *Food Chem. Toxicol.* **2009**, *47*, 1139.
- Yang, C.; Xu, L.; Zhou, Y.; Zhang, X.; Huang, X.; Wang, M.; Han, Y.; Zhai, M.; Wei, S.; Li, J. *Carbohydr. Polym.* **2010**, *82*, 1297.

30. Maia, J.; Ribeiro, P. M.; Ventura, C.; Carvalho, A. R.; Correia, I. J.; Gil, H. M. *Acta Biomater.* **2009**, *5*, 1948.
31. Martwiset, S.; Koh, E. A.; Chen, W. *Langmuir* **2006**, *22*, 8192.
32. Shazly, M. T.; Baker, B. A.; Naber, R. J.; Bon, A.; van Vliet, K. J.; Edelman, R. E. *J. Biomed. Mater. Res. A* **2010**, *95*, 1159.
33. Stammen, A. J.; Williams, S.; Ku, N. D.; Guldborg, E. R. *Biomaterials* **2001**, *22*, 799.
34. Fini, M.; Motta, A.; Torricelli, P.; Giavaresi, G.; Nicoli Aldini, N.; Tschon, M.; Giardino, R.; Migliaresi, C. *Biomaterials* **2005**, *26*, 3527.
35. Wang, J.; Valmikinathan, M. C.; Liu, W.; Laurencin, T. C.; Yu, X. *J. Biomed. Mater. Res. A* **2010**, *93*, 753.
36. Valmikinathan, M. C.; Hoffman, J.; Yu, X. *Mater. Sci. Eng. C* **2011**, *31*, 22.
37. Valmikinathan, M. C.; Defroda, S.; Yu, X. *Biomacromolecules* **2009**, *10*, 1084.
38. Maia, J.; Ferreira, L.; Carvalho, R.; Ramos, M. A.; Gil, H. M. *Polymer* **2005**, *46*, 9604.
39. Bouhadir, H. K.; Hausman, S. D.; Mooney, J. D. *Polymer* **1999**, *40*, 3575.
40. Zhou, Y.; Yang, D.; Ma, G.; Tan, H.; Jin, Y.; Nie, J. *Polym. Adv. Technol.* **2008**, *19*, 1133.
41. Liu, Y. T.; Lin, L. Y. *Acta Biomater.* **2010**, *6*, 1423.
42. Mizrahy, S.; Peer, D. *Chem. Soc. Rev.*, to appear.
43. Obeid, E.; Adams, M.; Newman, J. *J. Bone Joint Surg Br* **1994**, *76B*, 315.
44. Igwe, C. J.; Mikael, E. P.; Nukavarapu, P. S. *J. Tissue Eng. Regen. Med.*, **2012**, doi: 10.1002/term.1506.
45. des Rieux, A.; De Berdt, P.; Ansorena, E.; Ucakar, B.; Damien, J.; Schakman, O.; Audouard, E.; Bouzin, C.; Auhl, D.; Simon-Yarza, T.; Feron, O.; Blanco-Prieto, M. J.; Carmeliet, P.; Bailly, C.; Clotman, F.; Preat, V. *J. Biomed. Mater. Res. A* **2013**, doi: 10.1002/jbm.a.34915.
46. Yonet-Tanyeri, N.; Rich, H. M.; Lee, M.; Lai, H. M.; Jeong, H. J.; Devolder, J. R.; Kong, H. *Biomaterials* **2013**, *34*, 8416.
47. Ito, T.; Yeo, Y.; Highley, B. C.; Bellas, E.; Benitez, C. A.; Kohane, S. D. *Biomaterials* **2007**, *28*, 975.
48. Weng, L.; Pan, H.; Chen, W. *J. Biomed. Mater. Res. A* **2008**, *85*, 352.
49. Chen, G. X.; Wang, Z.; Liu, W. S.; Park, J. H. *Biomaterials* **2002**, *23*, 4609.
50. Benoit, D. S. W.; Anseth, S. K. *Acta Biomater.* **2005**, *1*, 461.
51. Wei, J.; Yoshinari, M.; Takemoto, S.; Hattori, M.; Kawada, E.; Liu, B.; Oda, Y. *J. Biomed. Mater. Res. B: Appl. Biomater.* **2007**, *81*, 66.
52. Mo, X.; Xu, C.; Kotaki, M.; Ramakrishna, S. *Biomaterials* **2004**, *25*, 1883.
53. Martin, J. W.; Herst, M. P.; Chia, E. W.; Harper, L. *J. Free Radic. Biol. Med.* **2009**, *47*, 616.
54. Aitken, J. R.; Gibb, Z.; Mitchell, A. L.; Lambourne, R. S.; Connaughton, S. H.; de Iulius, G. N. *Biol. Reprod.* **2012**, *87*, 110.
55. Park, H.; Temenoff, S. J.; Tabata, Y.; Caplan, I. A.; Mikos, G. A. *Biomaterials* **2007**, *28*, 3217.
56. Segura, T.; Chung, H. P.; Shea, D. L. *Biomaterials* **2005**, *26*, 1575.
57. Lü, S.; Liu, M.; Ni, B. *Chem. Eng. J.* **2010**, *160*, 779.
58. Kelner, A.; Schacht, H. E. *J. Controlled Release* **2005**, *101*, 13.
59. Cadee, J.; de Groot, C.; Jiskoot, W.; den Otter, W.; Hennink, W. *J. Controlled Release* **2002**, *78*, 1.
60. Jeong, B.; Bae, H. Y.; Kim, W. S. *J. Controlled Release* **2000**, *63*, 155.
61. Bezemer, J.; Radersma, R.; Grijpma, D.; Dijkstra, P.; Feijen, J.; van Blitterswijk, C. *J. Controlled Release* **2000**, *64*, 179.
62. Jain, A.; Jain, A.; Gulbake, A.; Shilpi, S.; Hurkat, P.; Jain, K. *S. Crit. Rev. Ther. Drug Carrier Syst.* **2013**, *30*, 293.
63. He, C.; Zhuang, X.; Tang, Z.; Tian, H.; Chen, X. *Adv. Healthcare Mater.* **2012**, *1*, 48.
64. Sivakumaran, D.; Maitl, D.; Oszustowicz, T.; Hoare, T. *J. Colloid Interf. Sci.* **2013**, *392*, 422.
65. Williams, C. E.; Toomey, R.; Alcantar, N. *J. Biomed. Mater. Res. A* **2012**, *100*, 3296.
66. Devi, N.; Maji, K. T. *AAPS Pharm. Sci. Tech.* **2009**, *10*, 1412.